Inorganic Chemistry
Article

Inorg. Chem. **2009**, *48*, 7593–7603 **7593**
DOI: 10.1021/ic9000957

Heteroleptic Arene Ruthenium Complexes Based on *meso*-Substituted Dipyrrins: Synthesis, Structure, Reactivity, and Electrochemical Studies

Mahendra Yadav, Ashish Kumar Singh, Biswajit Maiti, and Daya Shankar Pandey*

Department of Chemistry, Faculty of Science, Banaras Hindu University, Varanasi - 221 005 (U.P.), India

Received January 17, 2009

First examples of heteroleptic arene ruthenium complexes containing dipyrrin ligands with the general formulations $[(\eta^6\text{-arene})RuCl(L)]$ [(arene = C_6H_6, $C_{10}H_{14}$; L = 5-(4-cyanophenyl)-dipyrromethene, cydpm; 5-(4-nitrophenyl)-dipyrromethene, ndpm and 5-(4-benzyloxyphenyl)-dipyrromethene, bdpm] have been synthesized. The complexes $[(\eta^6\text{-}C_{10}H_{14})RuCl(L)]$ (L = ndpm and cydpm) reacted with NaN_3 and NH_4SCN to afford neutral mononuclear complexes $[(\eta^6\text{-}C_{10}H_{14})Ru(N_3)(L)]$ and $[(\eta^6\text{-}C_{10}H_{14})Ru(SCN)(L)]$. Their reactions with EPh_3 (E = P, As) and exobidentate ditopic P−P and N−N donor ligands, namely, bis-(diphenylphosphino)methane (dppm) and 4,4′-bipyridine (bpy) in the presence of $AgSO_3CF_3$ afforded cationic mono- and binuclear complexes $[(\eta^6\text{-}C_{10}H_{14})Ru(L)(EPh_3)]SO_3CF_3$, $[\{(\eta^6\text{-}C_{10}H_{14})Ru(L)\}_2(\mu\text{-dppm})](SO_3CF_3)_2$, and $[\{(\eta^6\text{-}C_{10}H_{14})Ru(L)\}_2(\mu\text{-bpy})](SO_3CF_3)_2$, respectively. The reaction products have been characterized by analytical and spectral studies. Molecular structures of the representative complexes $[(\eta^6\text{-}C_{10}H_{14})RuCl(cydpm)]$, $[(\eta^6\text{-}C_6H_6)RuCl(cydpm)]$, $[(\eta^6\text{-}C_{10}H_{14})RuCl(ndpm)]$, $[(\eta^6\text{-}C_{10}H_{14})Ru(N_3)(ndpm)]$, and $[(\eta^6\text{-}C_{10}H_{14})Ru(PPh_3)(ndpm)]SO_3CF_3$ have been determined crystallographically. Redox behavior of the complexes has been investigated by electrochemical studies. Emission spectral studies at room temperature suggested that the complexes under study are non-emissive.

Introduction

Dipyrromethenes have attracted sustained research interest over past couple of decades owing to their potential use as valuable precursor in the synthesis of dyes, porphyrins, porphyrin based biomimetic systems, diverse porphyrin building blocks, and as intermediates in porphyrin transformations.[1−5] Because of the presence of two nitrogen donor atoms in the planar dipyrrin unit, it provides a versatile motif for complexation to the metals and has emerged as a versatile ligand in coordination chemistry.[6] In this regard highly conjugated *meso*-substituted dipyrrins have drawn considerable current attention.[7,8] The ease of synthesis of *meso*-substituted dipyrrins from aldehydes via condensation with pyrrole followed by oxidation has made them very useful in the synthesis of homo- and heteroleptic complexes.[6,9,10] The extensive π-skeleton of the phenyl ring present as *meso*-substituents and two of the conjugated rigid pyrrole rings in dipyrrins enable them to behave as a better bidentate nitrogen donor ligands like 2,2′-bipyridine or 1,10-phenanthroline.

*To whom correspondence should be addressed. E-mail: dspbhu@bhu.ac.in. Phone: + 91 542 6702480. Fax: + 91 542 2368174.

(1) (a) Ulrich, G.; Goze, C.; Guardigli, M.; Roda, A.; Ziessel, R. *Angew. Chem., Int. Ed.* **2005**, *44*, 3694–3698. (b) Sazanovich, I. V.; Balakumar, A.; Muthukumaran, K.; Hindin, E.; Kirmaier, C.; Diers, J. R.; Lindsey, J. S.; Hindine, E.; Diers, J. R.; Bocian, D. F.; Holten, D. *Inorg. Chem.* **2003**, *42*, 6616–6628. (c) Muthukumaran, K.; Zaidi, S. H. H.; Yu, L.; Thamyongkit, P.; Calder, M. E.; Sharada, D. S.; Lindsey, J. S. *J. Porphyrins Phthalocyanines* **2005**, *9*, 745–759.

(2) (a) Smith K. M. In *The Porphyrin Handbook*; Kadish, K. M.; Smith, K. M.; Guilard, R.; Eds.; Academic Press: San Diego, CA, 2000; Vol. *1*, pp 1−43. (b) Paine, J. B., III In *The Porphyrins*; Dolphin, D., Eds.; Academic Press: New York, 1978; Vol. *1*, pp 101−234.

(3) Lindsey, J. S. In *Metalloporphyrin-Catalyzed Oxidations*; Montanari, F., Casella, L.; Eds.; Kluwer Academic Publishers: The Netherlands, 1994; pp 49−86.

(4) Lindsey, J. S. In *The Porphyrin Handbook*; Kadish, K. M., Smith, K. M., Guilard, R., Eds.; Academic Press: San Diego, CA, 2000; Vol. *1*, pp 45−118.

(5) (a) Falk H. *The Chemistry of Linear Oligopyrroles and Bile Pigments*; Springer-Verlag: Wien, 1989. (b) Harmjanz, M.; Gill, H. S.; Scott, M. J. *J. Am. Chem. Soc.* **2000**, *122*, 10476–0477.

(6) (a) Wood, T. E.; Thompson, A. *Chem. Rev.* **2007**, *107*, 1831–1861 and reference therein. (b) Chen, Q.; Dolphin, D. *Can. J. Chem.* **2002**, *80*, 1668–1675. (c) Shin, J. Y.; Dolphin, D.; Patrick, B. O. *Cryst. Growth Des.* **2004**, *4*, 659–661. (d) Cohen, S. M.; Halper, S. R. *Inorg. Chim. Acta* **2002**, *341*, 12–16. (e) Halper, S. R.; Malachowski, M. R.; Delaney, H. M.; Cohen, S. M. *Inorg. Chem.* **2004**, *43*, 1242–1249. (f) Halper, S. R.; Cohen, S. M. *Angew. Chem., Int. Ed.* **2004**, *43*, 2385–2388. (g) Sutton, J. M.; Rogerson, E.; Wilson, C. J.; Sparke, A. E.; Archibald, S. J.; Boyle, R. W. *Chem. Commun.* **2004**, 1328–1329.

(7) (a) Lee, C. H.; Lindsey, J. S. *Tetrahedron* **1994**, *50*, 11427–11440. (b) Littler, B. J.; Miller, M. A.; Hung, C. H.; Wagner, R. W.; O. Shea, D. F.; Boyle, P. D.; Lindsey, J. S. *J. Org. Chem.* **1999**, *64*, 1391–1396. (c) Laha, J. K.; Dhanalekshmi, S.; Taniguchi, M.; Ambroise, A.; Lindsey, J. S. *Org. Process Res. Dev.* **2003**, *7*, 799–812.

(8) (a) Brückner, C.; Karunaratne, V.; Rettig, S. J.; Dolphin, D. *Can. J. Chem.* **1996**, *74*, 2183–2193. (b) Wagner, R. W.; Lindsey, J. S. *Pure Appl. Chem.* **1996**, *68*, 1373–1380.

(9) (a) Falk, H.; Schoppe, G. *Monatsh. Chem.* **1990**, *121*, 67–76. (b) Loudet, A.; Burgess, K. *Chem. Rev.* **2007**, *107*, 4891–4932. (c) Smalley, S. J.; Waterland, M. R.; Telfer, S. G. *Inorg. Chem.* **2009**, *48*, 13–15.

(10) (a) Roomi, M. W. *Tetrahedron Lett.* **1974**, *15*, 1131–1132. (b) Murakami, Y.; Matsuda, Y.; Iiyama, K. *Chem. Lett.* **1972**, 1069–1072. (c) Brückner, C.; Zhang, Y.; Rettig, S. J.; Dolphin, D. *Inorg. Chim. Acta* **1997**, *263*, 279–286.

Published on Web 07/17/2009

Further, one can modulate properties of the dipyrrins by incorporating electron withdrawing/donating substituents which have a pronounced effect on electrochemical and optical properties.[11] In general electron-donating groups increase electron density on the ligand and redox processes take place at the more negative potential, while the opposite effect occurs in the presence of electron withdrawing groups. Numerous main group and transition metal homoleptic complexes, their photoluminescence and other properties along with MOF: metal-organic frameworks (MOFs) based on *meso*-substituted dipyrrins are well documented.[6a,9,10] While a number of heteroleptic dipyrrin complexes based on Pd(II), Hg(II), Rh(I), Cr(III), Co(II), and Cu(II) are reported in the literature, there is just one report dealing with ruthenium dipyrrin complexes.[9c] Furthermore, ruthenium(II) complexes containing both the dipyrrin and η^6-arene ligands have not yet been reported.

Ruthenium(II) complexes possessing η^6-cyclic hydrocarbon ligands are versatile and potentially valuable synthetic intermediates that have seen applications in diverse areas of organic syntheses.[12] Air-stable, water-soluble cationic arene ruthenium complexes find wide applications in many areas including homogeneous catalysis, polymeric materials, nanocages and nanoparticle precursors.[13] Arene ruthenium complexes are also being explored for their medicinal properties as anticancer agents.[14] The dimeric arene ruthenium complexes $[\{(\eta^6\text{-arene})RuCl(\mu\text{-}Cl)\}_2]$ (η^6-arene = benzene, *p*-cymene) undergo a rich variety of chemical transformations via intermediacy of the chloro bridge cleavage reactions leading to the formation of a series of interesting neutral and cationic mononuclear half-sandwich η^6-arene ruthenium complexes.[15] Despite its extensive chemistry, reactivity of the arene ruthenium complexes $[\{(\eta^6\text{-arene})RuCl(\mu\text{-}Cl)\}_2]$ with *meso*-substituted dipyrrins have not been explored.

Because of our interests in this area we became interested in developing the coordination chemistry of a new class of arene ruthenium complexes based on *meso*-substituted dipyrrins.[16] In this paper we report the reproducible synthesis, spectral properties, structural characterization, and reactivity of some heteroleptic arene ruthenium complexes $[(\eta^6\text{-arene})RuCl(L)]$ containing 5-(4-cyanophenyl)-dipyrromethene, 5-(4-nitrophenyl)-dipyrromethene, and 5-(4-benzyloxyphenyl)-dipyrromethene as co-ligands. Also, we present herein the synthesis and characterization of some bis-(diphenylphosphino)-methane (dppm), 4,4′-bipyridine (bpy), and azido bridged dinuclear complexes containing dipyrrin ligands.

Experimental Section

Reagents. All the synthetic manipulations were performed under nitrogen atmosphere in deaerated solvents. The solvents were purified rigorously following standard procedures prior to their use.[17] Silver trifluoromethanesulfonate, triphenylphosphine, triphenylarsine, bis-(diphenylphosphino)-methane, sodium azide, potassium thiocyanate, 4,4′-bipyridine, 1,3-cyclohexadiene, α-phellandrene, 2,3-dicloro-5,6-dicyano-1,4-benzoquinone (DDQ), 4-cyanobenzaldehyde, 4-bezyloxybenzaldehyde, 4-nitrobenzaldehyde, pyrrole, tetrabutylammonium perchlorate, and ruthenium(III) chloride hydrate (all Aldrich) were used as received without further purifications. The precursor complexes $[\{(\eta^6\text{-arene})RuCl(\mu\text{-}Cl)\}_2]$ (arene = C_6H_6, $C_{10}H_{14}$)[18] and ligands 5-(4-cyanophenyl)-dipyrromethane, 5-(4-nitrophenyl)-dipyrromethane, and 5-(4-benzyloxyphenyl)-dipyrromethane[19] were prepared and purified following literature procedures.

General Methods. Elemental analyses for C, H, and N were performed on Exeter Analytical Inc. Model CE-440 CHN analyzer. Infrared spectra in KBr pellets were acquired on a Varian 3100 FT-IR spectrometer. $^1H/^{13}C$ NMR spectra were recorded on a JEOL AL 300 MHz spectrometer at room temperature (RT) using $CDCl_3$ as solvent and TMS as an internal reference. Electronic and emission spectral data were acquired on a Shimadzu UV-1700 series and LS-45 Luminescence spectrophotometers, respectively. FAB mass spectra were obtained on a JEOL SX 102/Da-600 Mass Spectrometer. Cyclic voltammetric and spectroelectrochemical measurements were performed on a CHI 620c electrochemical analyzer. A glassy

(11) (a) Choi, S. H.; Kim, K.; Jeon, J.; Meka, B.; Bucella, D.; Pang, K.; Khatua, S.; Lee, J.; Churchill, D. G. *Inorg. Chem.* **2008**, *47*, 11071–11083. (b) Rawling, T.; Xiao, H.; Lee, S.-T.; Colbran, S. B.; McDonagh, A. M. *Inorg. Chem.* **2007**, *46*, 2805–2813. (c) Christendat, D.; David, M.-A.; Morin, S.; Lever, A. B. P.; Kadish, K. M.; Shao, J. *J. Porphyrins Phthalocyanines* **2005**, *9*, 626–636.

(12) (a) Bennett, M. A.; Bruce, M. I.; Matheson, T. W. In *Comprehensive Organometallic Chemistry*; Wilkinson, G., Stone, F. G. A., Abel, E. W., Eds.; Ser. 4; Pergamon Press: Oxford, U.K., 1982; p 796. (b) Le Bozec, H.; Touchard, D.; Dixneuf, P. H. *Adv. Organomet. Chem.* **1989**, *29*, 163–247. (c) Wong, E.; Giandomenico, C. M. *Chem. Rev.* **1999**, *99*, 2451–2466. (d) Housecroft, C. E. In *Comprehensive Coordination Chemistry II*; McCleverty, J. A., Meyer, T. J., Eds.; Ser.; Pergamon Press: Oxford, U.K., 2005; p 555. (e) Naota, T.; Takaya, H.; Murahashi, S. E. *Chem. Rev.* **1998**, *98*, 2599–2660. (f) Bruneau, C.; Dixnenf, P. H. *Ruthenium Catalysis and Fine Chemistry*; Springer: Berlin, 2004; pp 45−79.

(13) (a) Süss-Fink, G.; Therrien, B. *Organometallics* **2007**, *26*, 766–774. (b) Diaz-Alvarez, A. E.; Crochet, P.; Zablocka, M. C.; Duhayon, V.; Cadierno, J.; Gimeno, J.; Majoral, J. P. *Adv. Synth. Catal.* **2006**, *348*, 1671–1679. (c) Chérioux, F.; Therrien, B.; Süss-Fink, G. *Chem. Commun.* **2004**, *2*, 204–205. (d) Canivet, J.; Süss-Fink, G. *Green Chem.* **2007**, *93*, 91. (e) Ogo, S.; Uehara, K.; Abura, T.; Watanabe, Y.; Fukuzumi, S. *Organometallics* **2004**, *23*, 3047–3052. (f) Lidrissi, C.; Romerosa, A.; Saoud, M.; Serrano-Ruiz, M.; Gonsalvi, L.; Peruzzini, M. *Angew. Chem., Int. Ed.* **2005**, *44*, 2568–2572. (g) Therrien, B.; Süss-Fink, G.; Govindaswamy, P.; Renfrew, A. K.; Dyson, P. J. *Angew. Chem., Int. Ed.* **2008**, *47*, 3773–3776. (h) Brasey, T.; Scopelliti, R.; Severin, K. *Chem. Commun.* **2006**, *31*, 3308–3310. (i) Piotrowski, H.; Polborn, K.; Hilt, G.; Severin, K. *J. Am. Chem. Soc.* **2001**, *123*, 2699–2700. (j) Süss-Fink, G.; Mollwitz, B.; Therrien, B.; Dadras, M.; Laurenczy, G.; Meister, A.; Meister, G. *J. Clust. Sci.* **2007**, *18*, 87. (k) Johnson, C. A.; Sharma, S.; Subramaniam, B.; Borovik, A. S. *J. Am. Chem. Soc.* **2005**, *127*, 9698–9699.

(14) (a) Sava, G.; Alessio, E.; Bergamo, A.; Mestroni, G. In *Topics in Biological Inorganic Chemistry*; Clarke, M. J., Sadler, P. J., Eds.; Springer Verlag: Berlin, 1999; Vol. *1*, p 143. (b) Bergamo, A.; Zorzet, S.; Gava, B.; Sorc, A.; Alessio, E.; Iengo, E.; Sava, G. *Anticancer Drugs* **2000**, *11*, 665–672. (c) Yan, Y. K.; Melchart, M.; Habtemariam, A.; Sadler, P. J. *Chem. Commun.* **2005**, *38*, 4764–4770. (d) Chen, H.; Parkinson, J. A.; Morris, R. E.; Sadler, P. J. *J. Am. Chem. Soc.* **2003**, *125*, 173–186. (e) Jakupec, M. A.; Galanski, M.; Arion, V. B.; Hartinger, C. G.; Keppler, B. K. *Dalton Trans.* **2008**, 183–194. (f) Dyson, P. J.; Sava, G. *Dalton Trans.* **2006**, 1929–1933.

(15) (a) Marchetti, F.; Pettinari, C.; Pettinari, R.; Cerquetella, A.; Cingolani, A.; Chan, E. J.; Kozawa, K.; Skelton, B. W.; White, A. H.; Wanke, R.; Kuznetsov, M. L.; Martins, L. M. D. R. S.; Pombeiro, A. J. L. *Inorg. Chem.* **2007**, *46*, 8245–8247. (b) Tribo, R.; Munoz, S.; Pons, J.; Yanez, R.; Alvarez-Larena, A.; Piniella, J. F.; Ros, J. *J. Organomet. Chem.* **2005**, *690*, 4072–4079. (c) Pelagatti, P.; Bacchi, A.; Calbiani, F.; Carcelli, M.; Elviri, L.; Pelizzi, C.; Rogolino, D. *J. Organomet. Chem.* **2005**, *690*, 4602–4610. (d) Dez, J.; Gamasa, M. P.; Gimeno, J.; Lastra, E.; Villar, A. *Eur. J. Inorg. Chem.* **2006**, *1*, 78–87. (e) Csbai, F.; Joo, F.; Trzeciak, A. M.; Ziolkowski, J. J. *J. Organomet. Chem.* **2006**, *691*, 3371–3376. (f) Govindaswamy, P.; Carroll, P. J.; Mozharivskyj, Y. A.; Kollipara, M. R. *J. Organomet. Chem.* **2005**, *690*, 885–894.

(16) (a) Singh, S. K.; Trivedi, M.; Chandra, M.; Sahay, A. N.; Pandey, D. S. *Inorg. Chem.* **2004**, *43*, 8600–8608. (b) Singh, S. K.; Joshi, S.; Singh, A. R.; Saxena, J. K.; Pandey, D. S. *Inorg. Chem.* **2007**, *46*, 10869–10876.

(17) Perrin, D. D.; Armango, W. L. F.; Perrin, D. R. *Purification of Laboratory Chemicals*; Pergamon: Oxford, U.K., 1986.

(18) (a) Bennett, M. A.; Smith, A. K. *J. Chem. Soc., Dalton Trans.* **1974**, 233–241. (b) Bennett, M. A.; Huang, T. N.; Matheson, T. W.; Smith, A. K. *Inorg. Synth.* **1982**, *21*, 74–78.

(19) (a) Rao, P. D.; Dhanalekshmi, S.; Littler, B. J.; Lindsey, J. S. *J. Org. Chem.* **2000**, *65*, 7323–7344. (b) Gryko, D.; Lindsey, J. S. *J. Org. Chem.* **2000**, *65*, 2249–2252. (c) Brueckner, C.; Karunaratne, V.; Rettig, S. J.; Dolphin, D. *Can. J. Chem.* **1996**, *74*, 2182. (d) Lee, C. H.; Lindsey, J. S. *Tetrahedron.* **1994**, *50*, 11427–11440.

carbon working electrode, platinum wire auxiliary electrode, and Ag/Ag^+ reference electrode were used in a standard three-electrode configuration. Tetrabutylammonium perchlorate (TBAP) was used as a supporting electrolyte, and the solution concentration was about 10^{-3} M. A platinum gauze working electrode was used in the spectroelectrochemical experiments. Spectroelectrochemical studies were performed in acetonitrile/0.1 M Bu_4NClO_4 at 298 K using Oceanoptics Spectrasuite.

Synthesis of [(η^6-$C_{10}H_{14}$)RuCl(cydpm)] (1). DDQ (0.228 g, 1.0 mmol) dissolved in benzene (150 mL) was added slowly (over an hour) to a stirring solution of 5-(4-cyanophenyl)-dipyrromethane (0.247 g, 1.0 mmol) in $CHCl_3$ (150 mL) cooled in an ice bath. After thin-layer chromatography (TLC) examination revealed complete consumption of the starting material, the solvent was evaporated, and the resulting dark residue was dissolved in $CHCl_3$/MeOH (75 mL; 1:1 v/v). Triethylamine (0.75 mL) and [{(η^6-$C_{10}H_{14}$)RuCl(μ-Cl)}$_2$] (0.306 g, 0.50 mmol) dissolved in dichloromethane (5 mL) were added to this solution. The dark reaction mixture thus obtained was refluxed overnight. After cooling to RT it was concentrated to dryness under reduced pressure to afford a black solid. The crude product was charged on a flash column (20 × 3 cm, SiO_2; CH_2Cl_2/hexane). Second, a bright orange band was collected and concentrated to dryness to afford [(η^6-$C_{10}H_{14}$)RuCl(cydpm)]. Yield: 52% (0.268 g) Anal. Calcd for $C_{26}H_{24}ClN_3Ru$: C, 60.64; H, 4.70; N, 8.16%. Found: C, 60.62; H, 4.74: N, 8.12%. IR (cm^{-1}): 2227, 1948, 1720, 1557, 1447, 1376, 1343, 1249, 1206, 992, 891, 814, 766, 717, and 474. ^{1}H NMR (δ, ppm): 1.10 (d, 6H, J = 6.9 Hz), 2.24 (s, 3H), 2.40 (m, 1H), 5.30 (dd, 4H), 6.45 (d, 2H, J = 4.8 Hz), 6.49 (d, 2H, J = 4.8 Hz), 7.50 (d, 2H, J = 6.6 Hz), 7.71 (d, 2H, J = 8.1 Hz), 8.03 (s, 2H). ^{13}C NMR (75.45 MHz, δ, ppm): 18.60 (*C*-CH_3), 22.05 {CH(*C*H_3)$_2$}, 30.60 {*C*H(CH_3)$_2$}, 84.70 (C_6H_4), 100.49 (*C*-CH_3), 102.16 (*C*-CHMe$_2$), 112.28 (*C*≡N), 118.51, 119.00, 130.50−131.30, 134.22, 142.67, 143.44, 155.51 (dipyrrin). UV−vis. (CH_2Cl_2, λ_{max} nm, ε): 495 (2.41×10^4), 440 (2.29×10^4), 301 (1.09×10^4), 267 (1.22×10^4), 237 (2.77×10^4).

Synthesis of [(η^6-C_6H_6)RuCl(cydpm)] (2). Complex **2** was prepared following the above procedure for **1** except that [{(η^6-C_6H_6)RuCl(μ-Cl)}$_2$] was used in place of [{(η^6-$C_{10}H_{14}$)-RuCl(μ-Cl)}$_2$]. Yield 54% (0.248 g). Anal. Calcd for $C_{22}H_{16}$-ClN_3Ru: C, 57.58; H, 3.51; N, 9.16%. Found: C, 57.54; H, 3.39: N, 9.12%. IR (cm^{-1}): 2227, 1648, 1556, 1460, 1378, 1341, 1245, 1195, 1033, 993, 889, 807, 722, 670, 528, and 473. ^{1}H NMR (δ, ppm); 5.68 (s, 6H), 6.46 (d, 2H, J = 3.9 Hz), 6.51 (d, 2H, J = 3.3 Hz), 7.51 (d, 2H, J = 6.6 Hz), 7.70 (d, 2H, J = 8.1 Hz), 8.15 (s, 2H) .UV−vis. (CH_2Cl_2, λ_{max} nm, ε): 495 (2.50×10^4), 442 (1.34×10^4), 302 (1.01×10^4), 268 (1.22×10^4), 236 (2.85×10^4).

Synthesis of [(η^6-$C_{10}H_{14}$)RuCl(ndpm)] (3). It was prepared following the method for **1** except that 5-(4-nitrophenyl) dipyrromethane (0.267 g, 1.0 mmol) was used in place of 5-(4-cyanophenyl)-dipyrromethane. Yield: 54% (0.289 g). Anal. Calcd for $C_{25}H_{24}ClN_3O_2Ru$: C, 56.13; H, 4.52: N, 7.85%. Found: C, 56.09; H, 4.48; N, 7.79%. IR (cm^{-1}): 1555, 1519, 1471, 1376, 1344, 1247, 1102, 1027, 992, 893, 822, 720, and 477. ^{1}H NMR (δ, ppm): 1.10 (d, 6H, J = 6.9 Hz), 2.25 (s, 3H), 2.46 (m, 1H), 5.31 (dd, 4H), 6.45 (d, 2H, J = 3.9 Hz), 6.49 (d, 2H, J = 4.2 Hz), 7.55 (d, 2H, J = 8.4 Hz), 8.04 (s, 2H), 8.27 (d, 2H, J = 8.7 Hz). ^{13}C NMR (75.45 MHz, δ, ppm): 18.62 (*C*-CH_3), 22.07 {CH(*C*H_3)$_2$}, 30.63 {*C*H(CH_3)$_2$}, 84.73 (C_6H_4), 100.51 (*C*-CH_3), 102.25 (*C*-CHMe$_2$), 119.10, 122.55, 130.61, 131.63, 134.16, 143.02, 144.57, 147.85, 155.62 (dipyrrin). UV−vis. (CH_2Cl_2, λ_{max} nm, ε): 498 (2.37×10^4), 446 (1.61×10^4), 303 (1.41×10^4), 272 (1.86×10^4), 237 (1.63×10^4).

Synthesis of [(η^6-C_6H_6)RuCl(ndpm)] (4). Complex **4** was synthesized following the method employed for **1** using 5-(4-nitrophenyl) dipyrromethane (0.267 g, 1.0 mmol) and [{(η^6-C_6H_6)RuCl(μ-Cl)}$_2$]. Yield: 53% (0.254 g). Anal. Calcd for $C_{21}H_{16}ClN_3O_2Ru$: C, 52.67; H, 3.37; N, 8.77%. Found: C, 52.62; H, 3.31: N, 8.73%. IR (cm^{-1}): 1555, 1378, 1343, 1246, 1145, 1034, 995, 893, 821, 786, 736, and 478. ^{1}H NMR (δ, ppm): 5.69 (s, 6H), 6.47 (d, 2H, J = 4.5 Hz), 6.52 (d, 2H, J = 3.6 Hz), 7.60 (d, 2H, J = 8.4 Hz), 8.16 (s, 2H), 8.27 (d, 2H, J = 8.4 Hz). UV−vis. (CH_2Cl_2, λ_{max} nm, ε): 497 (2.52×10^4), 441 (1.18×10^4), 301 (1.31×10^4), 273 (1.71×10^4), 228 (1.51×10^4).

Synthesis of [(η^6-$C_{10}H_{14}$)RuCl(bdpm)] (5). This complex was prepared following the above procedure for **1** except that 5-(4-benzyloxyphenyl)-dipyrromethane was used in place of 5-(4-cyanophenyl)-dipyrromethane (0.328 g, 1.0 mmol). Yield: 50% (0.298 g). Anal. Calcd for $C_{32}H_{31}ClN_2ORu$: C, 64.47; H, 5.24; N, 4.70%. Found: C, 64.35; H, 5.30; N, 4.68%. IR (cm^{-1}): 1708, 1603, 1547, 1460, 1380, 1342, 1244, 1171, 997, 796, 733, 699, and 472. ^{1}H NMR (δ, ppm): 1.09 (d, 6H, J = 6.9 Hz), 2.22 (s, 3H), 2.45 (m, 1H), 5.27 (dd, 4H), 5.12 (s, 2H), 6.47 (d, 2H, J = 3.9 Hz), 6.64 (d, 2H, J = 4.5 Hz), 6.99 (d, 2H, J = 8.1 Hz), 7.32−7.48 (m, 7H), 7.99 (s, 2H). ^{13}C NMR (75.45 MHz, δ, ppm): 18.57 (*C*-CH_3), 22.07 {CH(*C*H_3)$_2$}, 30.54 {*C*H(CH_3)$_2$}, 70.09 (−*C*H_2−Ph), 84.68 (C_6H_4), 100.17 (*C*-CH_3), 102.00 (*C*-CHMe$_2$), 113.51, 118.14, 127.54, 128.07, 128.63, 130.83, 131.80, 135.37, 136.75, 146.40, 154.55, 159.05 (dipyrrin). UV−vis. (CH_2Cl_2, λ_{max} nm, ε): 493 (2.52×10^4), 440 (1.72×10^4), 350 (1.17×10^4), 271 (1.19×10^4), 233 (3.05×10^4).

Synthesis of [(η^6-$C_{10}H_{14}$)Ru(N_3)(cydpm)] (6). Complex **1** (0.515 g, 1.0 mmol) in dry acetone (20 mL) was treated with sodium azide NaN_3 (0.065 g, 1.0 mmol), and the suspension was stirred at RT for 3 h. It was concentrated to dryness under reduced pressure, extracted with dichloromethane (10 mL) and filtered to remove solid sodium chloride. The filtrate was concentrated to ∼2 mL, and an excess of hexane was added to it. The orange colored microcrystalline compound thus obtained was filtered, washed with diethyl ether, and dried under vacuum. Yield: 79% (0.412 g). Anal. Calcd for $C_{26}H_{24}N_6Ru$: C, 59.87; H, 4.64; N, 16.11%. Found: C, 59.70; H, 4.56; N, 16.15%. IR (cm^{-1}): 2226, 2025, 1707, 1555, 1460, 1378, 1342, 1246, 1031, 993, 893, 812, 769, 720, and 474. ^{1}H NMR (δ, ppm): 1.06 (d, 6H, J = 6.6 Hz), 2.17 (s, 3H), 2.38 (m, 1H), 5.27 (d, 2H, J = 6.3 Hz), 5.42 (d, 2H, J = 6.6 Hz), 6.44 (d, 2H, J = 3.9 Hz), 6.50 (d, 2H, J = 3.6 Hz), 7.49 (d, 2H, J = 8.1 Hz), 7.71 (d, 2H, J = 8.1 Hz), 8.04 (s, 2H). UV−vis. (CH_2Cl_2, λ_{max} nm, ε): 490 (2.40×10^4), 300 (1.21×10^4), 265 (1.50×10^4), 236 (3.01×10^4).

Synthesis of [(η^6-$C_{10}H_{14}$)Ru(SCN)(cydpm)] (7). This complex was prepared following the above procedure for **6** using NH_4SCN in place of NaN_3. Yield: 75% (0.403 g). Anal. Calcd for $C_{27}H_{24}N_4SRu$: C, 60.32; H, 4.50; N, 10.42%. Found: C, 60.28; H, 4.48; N, 10.37%. IR (cm^{-1}): 2227, 2100, 1708, 1553, 1459, 1378, 1342, 1246, 1229, 992, 893, 813, 769, 719, and 471. ^{1}H NMR (δ, ppm): 1.08 (d, 6H, J = 6.6 Hz), 2.17 (s, 3H), 2.37 (m, 1H), 5.34 (d, 2H, J = 6.0 Hz), 5.40 (d, 2H, J = 6.0 Hz), 6.47 (dd, 4H), 7.49 (d, 2H, 8.4 Hz), 7.72 (d, 2H, J = 8.1 Hz), 7.94 (s, 2H) . UV−vis. (CH_2Cl_2, λ_{max} nm, ε): 486 (2.40×10^4), 300 (1.26×10^4), 266 (1.53×10^4), 237 (2.98×10^4).

Synthesis of [(η^6-$C_{10}H_{14}$)Ru(PPh_3)(cydpm)]SO_3CF_3 (8). Complex **1** (0.515 g, 1.0 mmol) in dry acetone (30 mL) was treated with $AgSO_3CF_3$ (0.257 g, 1 mmol) and stirred for 2 h at RT. It was filtered through Celite to remove silver chloride. Triphenylphosphine (0.262 g, 1 mmol) was added to the filtrate and stirred at RT for 4 h. The solvent was removed under reduced pressure and residue extracted with dichloromethane (5 mL) and filtered. An excess of hexane was added to the filtrate to afford a yellow colored precipitate. It was separated by filtration, washed with diethyl ether, and dried under vacuum. Yield: 68%(0.606 g). Anal. Calcd for $C_{45}H_{39}N_3O_3F_3PSRu$: C, 60.67; H, 4.41; N, 4.72%. Found: C, 60.49; H, 4.53; N, 4.68%. IR (cm^{-1}): 2223, 1558, 1473, 1437, 1382, 1345, 1253, 1156, 1092, 1030, 993, 892, 812, 752, 698, 635, 569, and 517. ^{1}H NMR (δ, ppm): 0.92 (d, 6H, J = 6.6 Hz), 1.68 (s, 3H), 2.18 (m, 1H), 5.90 (d, 2H, J = 5.7 Hz), 6.01 (d, 2H, J = 6.3 Hz), 6.29 (d, 2H, J = 3.9 Hz), 6.38 (d, 2H, J = 3.9 Hz), 7.43−7.02 (m, 17H), 7.70 (d, 2H, J = 8.1 Hz), 7.96 (s, 2H). ^{31}P{^{1}H} NMR (121.50 MHz,

δ, ppm): 40.38 (P, PPh_3). UV−vis. (CH_2Cl_2, λ_{max} nm, ε): 498 (2.42×10^4), 438 (0.83×10^4), 309 (1.12×10^4), 242 (2.51×10^4).

Synthesis of [(η^6-$C_{10}H_{14}$)Ru(ndpm)N_3] (9). This complex was prepared following the procedure adopted for **6** using complex **3** (0.535 g, 1.0 mmol) in place of **1**. Yield: 84% (0.454 g). Anal. Calcd for $C_{25}H_{24}N_6O_2Ru$: C, 55.44; H, 4.47; N, 15.52%. Found: C, 55.00; H, 4.39; N, 15.55%. IR (cm^{-1}): 2025, 1556, 1502, 1464, 1378, 1341, 1246, 1099, 1031, 994, 897, 822, 725, and 477. ^{1}H NMR (δ, ppm): 1.05 (d, 6H, J = 6.6 Hz), 2.28 (s, 3H), 2.44 (m, 1H), 5.27 (d, 2H, J = 5.1 Hz), 5.37 (d, 2H, J = 5.1 Hz), 6.48 (d, 2H, J = 4.2 Hz), 6.53 (d, 2H, J = 4.5 Hz), 7.55 (d, 2H, J = 8.4 Hz), 8.02 (s, 2H), 8.26(d, 2H, J = 8.7 Hz). UV−vis. (CH_2Cl_2, λ_{max} nm, ε): 489 (2.36×10^4), 305 (2.18×10^4), 273 (2.31×10^4), 232 (2.51×10^4).

Synthesis of [(η^6-$C_{10}H_{14}$)Ru(SCN)(ndpm)] (10). This complex was prepared from [(η^6-$C_{10}H_{14}$)RuCl(ndpm)] (0.535 g, 1.0 mmol) and NH_4SCN (0.076 g, 1.0 mmol) following the method employed for **7**. Yield: 84% (0.467 g). Anal. Calcd for $C_{26}H_{24}N_4O_2SRu$: C, 56.00; H, 4.34; N, 10.05% Found: C, 56.08; H, 4.30 ; N, 10.08%. IR (cm^{-1}): 2100, 1552, 1521, 1377, 1344, 1246, 1096, 1030, 993, 893, 822, 719, and 476. ^{1}H NMR (δ, ppm): 1.12 (d, 6H, J = 6.9 Hz), 2.21 (s, 3H), 2.38 (m, 1H), 5.38 (dd, 4H), 6.50 (s, 4H), 7.56 (bs, 2H), 7.88 (s, 1H), 7.95 (s, 1H), 8.29 (s, 2H). UV−vis. (CH_2Cl_2, λ_{max} nm, ε): 495 (2.35×10^4), 444 (1.45×10^4), 304 (1.53×10^4), 267 (2.20×10^4), 231 (2.57×10^4).

Synthesis of [(η^6-$C_{10}H_{14}$)Ru(PPh_3)(ndpm)]SO_3CF_3 (11). It was prepared following the method employed for **8** using the complex [(η^6-$C_{10}H_{14}$)RuCl(ndpm)] (0.535 g, 1.0 mmol). Yield: 70% (0.637 g). Anal. Calcd for $C_{44}H_{39}N_3O_5F_3PSRu$: C, 58.02; H, 4.32; N, 4.61%. Found: C, 58.04; H, 4.28; N, 4.58%. IR (cm^{-1}): 1597, 1556, 1521, 1477, 1437, 1382, 1348, 1262, 1159, 1093, 1033, 994, 892, 824, 748, 700, 637, and 530. ^{1}H NMR (δ, ppm): 0.95 (d, 6H, J = 6.6 Hz), 1.69 (s, 3H), 2.26 (m, 1H), 5.90 (d, 4H, J = 6.0 Hz), 6.02 (d, 2H, J = 6.3 Hz), 6.31 (d, 2H, J = 3.9 Hz), 6.34 (d, 2H, J = 4.5 Hz), 7.11−7.46 (m, 17H), 7.98 (s, 2H), 8.25 (d, 2H, J = 8.7 Hz). ^{31}P{^{1}H} NMR (121.50 MHz, δ, ppm): 41.68 (P, PPh_3) UV−vis. (CH_2Cl_2, λ_{max} nm, ε): 495 (2.39×10^4), 436 (0.74×10^4), 308 (1.00×10^4), 258 (2.51×10^4), 232 (2.54×10^4).

Synthesis of [(η^6-$C_{10}H_{14}$)Ru($AsPh_3$)(ndpm)]SO_3CF_3 (12). It was prepared following the above procedure using [(η^6-$C_{10}H_{14}$)RuCl(ndpm)] (0.535 g, 1.0 mmol) and $AsPh_3$ (0.109 g, 1.0 mmol). Yield: 68% (0.649 g). Anal. Calcd for $C_{44}H_{39}N_3O_5F_3AsSRu$: C, 55.35; H, 4.12; N, 4.40%. Found: C, 55.32; H, 4.09; N, 4.37%. IR (cm^{-1}): 1555, 1383, 1346, 1260, 1154, 1031, 995, 826, 742, 635, and 474. ^{1}H NMR (δ, ppm): 0.94 (d, 6H, J = 6.9 Hz), 1.85 (s, 3H), 2.29 (m, 1H), 6.00 (d, 2H, J = 6.0 Hz), 6.07 (d, 2H, J = 6.0 Hz), 6.28 (d, 2H, J = 4.5 Hz), 6.45 (d, 2H, J = 3.9 Hz), 7.19−7.45 (m, 17H), 8.12 (s, 2H), 8.22 (t, 2H, J = 6.0 Hz). UV−vis. (CH_2Cl_2, λ_{max} nm, ε): 495 (2.39×10^4), 438 (0.76×10^4), 306 (1.19×10^4), 262 (2.52×10^4), 231 (2.55×10^4).

Synthesis of [{(η^6-$C_{10}H_{14}$)Ru(ndpm)}$_2$(μ-dppm)]$(SO_3CF_3)_2$ (13). Complex **13** was prepared following the above procedure using [(η^6-$C_{10}H_{14}$)RuCl(ndpm)] (0.535 g, 1.0 mmol) and dppm (0.192 g, 0.50 mmol). Yield: 62% (0.521 g). Anal. Calcd for $C_{77}H_{70}N_6O_{10}F_6P_2S_2Ru_2$: C, 55.00; H, 4.20; N, 5.00%. Found: C, 54.97; H, 4.16; N, 5.04%. IR (cm^{-1}): 1556, 1436, 1382, 1347, 1259, 1157, 1102, 1031, 993, 827, 742, 704, 637, 512, and 478. ^{1}H NMR (δ, ppm): 0.93 (d, 12H, J = 4.2 Hz), 2.18 (s, 6H), 2.32 (m, 2H), 3.18 (s, 2H), 5.88−5.71 (m, 8H), 6.52−6.48 (m, 8H), 6.90−7.65 (m, 24H), 8.09 (s, 4H), 8.32 (dd, 4H). UV−vis. (CH_2Cl_2, λ_{max} nm, ε): 491 (2.37×10^4), 434 (1.08×10^4), 304 (0.92×10^4), 258 (1.93×10^4), 248 (2.01×10^4).

Synthesis of [{(η^6-$C_{10}H_{14}$)Ru(ndpm)}$_2$(μ-bpy)]$(SO_3CF_3)_2$ (14). Complex **14** was prepared following the above procedure using [(η^6-$C_{10}H_{14}$)RuCl(ndpm)] (0.535 g, 1.0 mmol) and 4,4′-bpy (0.078 g, 0.50 mmol). Yield: 65% (0.472 g). Anal. Calcd for $C_{62}H_{56}N_8O_{10}F_6S_2Ru_2$: C, 51.24; H, 3.88; N, 7.71%. Found: C, 51.16; H, 3.81; N, 7.76%. IR (cm^{-1}): 1556, 1436, 1382, 1347, 1259, 1157, 1102, 1031, 993, 827, 742, 704, 637, 512, and 478. ^{1}H NMR (δ, ppm): 1.01 (d, 12H, J = 6.6 Hz), 1.83 (s, 6H), 2.36 (m, 2H), 5.30 (s, 8H), 5.85 (d, 2H, J = 6.0 Hz), 5.94 (d, 2H, J = 5.7 Hz), 6.46 (d, 4H, J = 3.9 Hz), 6.68 (d, 4H, J = 4.2 Hz), 7.45 (d, 2H, J = 6.0 Hz), 7.60 (bs, 2H), 7.72 (d, 4H, J = 6.0 Hz), 8.20 (d, 2H, J = 3.9 Hz), 8.41 (d, 2H, J = 4.2 Hz), 8.48 (bs, 2H), 8.52 (d, 2H, J = 6.6 Hz). UV−vis. (CH_2Cl_2, λ_{max} nm, ε): 496 (2.49×10^4), 424 (1.48×10^4), 302 (1.97×10^4), 266 (2.32×10^4).

Synthesis of [{(η^6-$C_{10}H_{14}$)Ru(cydpm)}$_2$(μ-N_3)]Cl (15). To a suspension of complex **1** (0.515 g, 1.0 mmol) in dry acetone (15 mL) sodium azide NaN_3 (0.033 g, 0.5 mmol) was added and stirred for 3 h at RT. The solvent was removed under reduced pressure, and residue extracted with dichloromethane (10 mL) and filtered to remove solid sodium chloride. The filtrate was concentrated to ~2 mL and an excess of hexane was added to it. An orange colored complex separated which was filtered, washed with diethyl ether, and dried under vacuum. Yield 79% (0.425 g). Anal. Calcd for $C_{50}H_{48}ClN_9O_4Ru_2$: C, 55.78; H, 4.49; N, 11.78%. Found: C, 55.72; H, 4.46; N, 11.71%. IR (cm^{-1}): 2226, 2026, 1705, 1555, 1462, 1379, 1342, 1247, 1031, 993, 893, 812, 770, 721, and 474. ^{1}H NMR (δ, ppm): 1.05 (d, 12H, J = 6.9 Hz), 2.24 (s, 6H), 2.43 (m, 2H), 5.26 (d, 4H, J = 6.0 Hz), 5.36 (d, 4H, J = 6.3 Hz), 6.46 (d, 4H, J = 3.6 Hz), 6.52 (d, 4H, J = 4.2 Hz), 7.50 (d, 4H, J = 8.4 Hz), 7.70 (d, 4H, J = 8.1 Hz), 8.01 (s, 4H). UV−vis. (CH_2Cl_2, λ_{max} nm, ε): 486 (2.41×10^4), 302 (1.19×10^4), 268 (1.50×10^4), 234 (3.13×10^4).

X-ray Structure Determinations. Crystals suitable for single crystal X-ray diffraction analyses for **1**, **2**, **3**, **9**, and **11** were grown by slow diffusion of hexane in dichloromethane solution of the respective compounds. Preliminary data on the space group and unit cell dimensions as well as intensity data for **2**, **9**, and **11** were collected on Oxford Diffraction Xcalibur-S and on a Bruker Smart Apex diffractometer for **1** and **3** using graphite monochromatized Mo Kα radiation. The structures were solved by direct methods and refined by using SHELX-97.[20] Non-hydrogen atoms were refined with anisotropic thermal parameters. All the hydrogen atoms were geometrically fixed and allowed to refine using a riding model. PLATON was used for analyzing the interaction and stacking distances.[20]

Results and Discussion

Syntheses of the Ligands and Complexes 1−5. One pot reaction of aldehyde with an excess of pyrrole at RT offers a suitable route for the synthesis of *meso*-substituted dipyrromethanes.[7] In our systematic studies on the possibility of binding of the dipyrrinato ligands to metal centers we have prepared and characterized various Ru(II) complexes. In a typical reaction, dipyrromethanes were oxidized to the corresponding dipyrrin by reaction of the respective dipyrromethane with DDQ in a chloroform/benzene solution. The dipyrrin ligands were not isolated, rather these were used in situ to generate the desired complexes.[6d,8a,10c,21,22] Neutral heteroleptic complexes with the formulations [(η^6-arene)Ru(L)Cl] were obtained by treatment of the dipyrrins with arene ruthenium complexes [{(η^6-arene)RuCl(μ-Cl)}$_2$] (arene = C_6H_6, $C_{10}H_{14}$) in the presence of triethylamine under refluxing conditions. A simple scheme showing synthesis of the complexes **1**−**5** is depicted in Scheme 1. These are

(20) (a) Mackay, S.; Dong, W.; Edwards, C.; Henderson, A.; Gilmox, C.; Stewart, N.; Shankland, K.; Donald, A. *MAXUS*; University of Glasgow: Scotland, 1999. (b) Sheldrick, G. M. *SHELX-97, Programme for refinement of crystal structures*; University of Gottingen: Gottingen, Germany, 1997. (c) *PLATON*; Spek, A. L. *Acta Crystallogr. A* 1990, *46*, C31.

(21) Halper, S. R.; Cohen, S. M. *Chem.—Eur. J.* **2003**, *9*, 4661–4669.

(22) Yu, L. H.; Muthukumaran, K.; Sazanovich, I. V.; Kirmaier, C.; Hindin, E.; Diers, J. R.; Boyle, P. D.; Bocian, D. F.; Holten, D.; Lindsey, J. S. *Inorg. Chem.* **2003**, *42*, 6629–6647.

Scheme 1

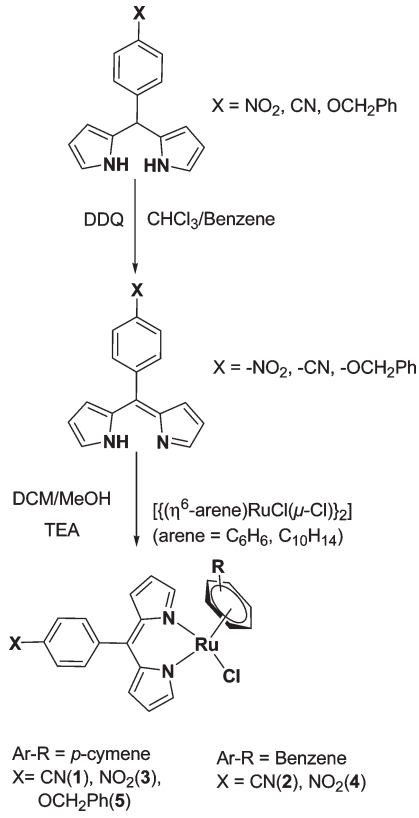

bright orange-red compounds that generally appear lustrous green upon removal of the solvent and are stable toward air and moisture. The complexes readily dissolve in common organic solvents such as chloroform, dichloromethane, acetone, acetonitrile, dimethylformamide, and dimethylsulfoxide.

Crystallographic Studies. Molecular structures of the complexes **1**−**3** have been determined crystallographically. Crystallographic data and selected geometrical parameters for **1**−**3** are summarized in Table 1 and 2. Oak Ridge Thermal Ellipsoid Plot (ORTEP) views with the atom-numbering scheme (30% probability) are shown in Figure 2. The dipyrrin ligands in these complexes are coordinated to metal center in an analogous manner as observed in other dipyrrinato complexes.[6f,8a,21,23] Coordination geometry about the metal center ruthenium in **1**−**3** is typical "*piano-stool*" geometry with two positions occupied by dipyrrin nitrogen, one chloro group and arene rings (arene = $C_{10}H_{14}$, **1** and **3**; C_6H_6, **2**) bonded in η^6-manner.

The *piano-stool* arrangement about ruthenium center is further reflected by small bite angles of dpm [N(1)−Ru(1)−N(2) 84.86(12)° (**1**), N(1)−Ru(1)−N(2) 86.79(9)° (**2**), and N(1)−Ru(1)−N(2) 85.70(17)° (**3**)].[23] Arene rings in these complexes are normal with an average Ru−C distances of 2.194 (**1**), 2.179 (**2**), and 2.196 Å (**3**), respectively. The metal to arene ring centroid separations are 1.675 (**1**), 1.682 (**2**), and 1.678 (**3**) Å. These separations are shorter than those reported in other arene ruthenium complexes.[16,24] and may be attributed to enhanced back-bonding. The pyrrole rings of dipyrrin are not coplanar and *meso*-phenyl rings are twisted out of the methene plane by 113.3(4) (**1**), 91.0(4) (**2**), and 70.3(7)° (**3**), and consequently there are major differences in crystal packing. The Ru1 to dpm nitrogen bond lengths Ru1−N1 and Ru1−N2 are 2.077(3) and 2.075(3) Å in **1**, 2.081(2) and 2.081(2) Å in **2**, and 2.075(4) and 2.070(4) Å in **3**.[25] The Ru−Cl distances are 2.4226(8), 2.4194(8), and 2.3982(15) Å in **1**, **2**, and **3**, respectively. These are consistent with the values reported in other related complexes.[15,16,24]

Weak interaction studies on the complex [(η^6-C_6H_6)-RuCl(cydpm)] **2** revealed an interesting structural features. In the crystal packing two molecules of [(η^6-C_6H_6)RuCl(cydpm)] are involved in $\pi-\pi$ stacking, resulting in a dimeric structure with centroid−centroid separation of 3.649 Å. Observed distances are consistent with the theoretical value calculated for $\pi-\pi$ stacking.[26] The C−H···Cl and C−H···O [Supporting Information, Table S1] interactions in **2** and **3** lead to various structural motifs shown in the Supporting Information, Figures S10−S12, S14. It is well established that these types of interactions play an important role in the construction of huge supramolecular architectures.[15,27]

Syntheses and Characterization of Substituted Derivatives of 1 and 3. Space-filling representations of [(η^6-$C_{10}H_{14}$)RuCl(cydpm)] **1** and [(η^6-$C_{10}H_{14}$)RuCl(ndpm)] **3** (Figure 1) indicated that the coordination geometry about metal center ruthenium provides an open face for facile replacement of the chloro group by other ligands. It prompted us to examine the reactivity of the complexes **1** and **3** with some nitrogen and phosphorus donor ligands. It was observed that reactions of the complexes **1** and **3** with anionic ligands like N_3^- or SCN^- in acetone led in the formation of neutral complexes [(η^6-$C_{10}H_{14}$)Ru-(cydpm)N_3] **6**, [(η^6-$C_{10}H_{14}$)Ru(cydpm)SCN] **7**, [(η^6-C_{10}-H_{14})Ru(ndpm)N_3] **9**, and [(η^6-$C_{10}H_{14}$)Ru(ndpm)SCN] **10**. On the other hand, reactions with neutral ligands like EPh_3 (P, As) or exobidantate ligands dppm or 4,4′-bpy in the presence of $AgSO_3CF_3$ afforded cationic mononuclear complexes [(η^6-$C_{10}H_{14}$)Ru(PPh_3)(cydpm)]SO_3CF_3 **8**, [(η^6-$C_{10}H_{14}$)Ru(PPh_3)(ndpm)SO_3CF_3 **11**, [(η^6-$C_{10}H_{14}$)Ru-($AsPh_3$)(ndpm)]SO_3CF_3 **12**, and binuclear complexes [{(η^6-$C_{10}H_{14}$)Ru(ndpm)}$_2$(μ-dppm](SO$_3$-CF_3)$_2$ **13**, [{(η^6-$C_{10}H_{14}$)Ru(ndpm)}$_2$(μ-bpy)](SO_3CF_3)$_2$ **14**. Further, it was observed that reaction of **1** with NaN_3 under controlled conditions afforded a binuclear complex with the formulation [{(η^6-$C_{10}H_{14}$)Ru(cydpm)}$_2$(μ-N_3)]Cl **15**. A simple scheme showing synthesis of the derivatives of **1** and **3** is depicted in Scheme 2.

IR spectra of the complexes **6** and **7** exhibited an insignificant shift in the position of bands associated with ν(C≡N) at ∼2227 cm^{-1} and the appearance of additional bands at ∼2025 and ∼2100 cm^{-1}, respectively,

(23) (a) Gill, H. S.; Finger, I.; Bozidarevic, I.; Szydlo, F.; Scott, M. J. *New J. Chem.* **2005**, *29*, 68–71. (b) Do, L.; Halper, S. R.; Cohen, S. M. *Chem. Commun.* **2004**, 2662–2663.

(24) (a) Singh, A.; Chandra, M.; Sahay, A. N.; Pandey, D. S.; Pandey, K. K.; Mobin, S. M.; Puerta, M. C.; Valerga, P. *J. Organomet. Chem.* **2004**, *68*, 1821–1834. (b) Clear, J. M.; O'Connell, C. M.; Vos, J. G.; Cardin, C. J.; Edwards, A. J. *J. Chem. Soc., Chem. Commun.* **1980**, 750–751.

(25) Thoi, V. S.; Stork, J. R.; Magde, D.; Cohen, S. M. *Inorg. Chem.* **2006**, *45*, 10688–10697.

(26) (a) Scaccianoce, L.; Braga, D.; Calhorda, M. J.; Grepioni, F.; Johnson, B. F. G. *Organometallics* **2000**, *19*, 790–797. (b) Tsuzuki, S.; Honda, K.; Uchimura, T.; Mikami, M.; Tanabe, K. *J. Am. Chem. Soc.* **2004**, *124*, 104–112.

(27) Severin, K. *Chem. Commun.* **2006**, 3859–3867.

Table 1. Crystal Data and Structure Refinement Parameters for **1**, **2**, **3**, **9**, and **11**

	1	**2**	**3**	**9**	**11**
empirical formula	$C_{26}H_{24}N_3ClRu$	$C_{22}H_{16}N_3ClRu$	$C_{25}H_{24}N_3O_2ClRu$	$C_{25}H_{24}N_6O_2Ru$	$C_{44}H_{39}N_3PO_5SRu$
crystal system	triclinic	monoclinic	triclinic	triclinic	monoclinic
space group	$P\bar{1}$	$P21/n$	$P\bar{1}$	$P\bar{1}$	$P21/c$
a (Å)	9.6577(6)	13.1357(3)	14.860(3)	9.9452(4)	20.2148(4)
b (Å)	10.4759(6)	7.3731(1)	16.732(3)	9.9780(3)	12.6772(2)
c (Å)	11.9408(7)	19.0071(5)	17.731(3)	11.5966(3)	16.3008(3)
α (deg)	73.9480(10)	90.00	108.592(3)	104.577(2)	90.00
β (deg)	77.9880(10)	101.851(2)	101.479(3)	91.193(3)	101.722(2)
γ(deg)	83.9790(10)	90.00	109.477(3)	92.054(3)	90.00
V (Å^3), Z	1134.12(12), 2	1801.62(7), 4	3702.4(12), 2	1112.48(6), 2	4090.24(13), 4
λ (Å)	0.71073	0.71073	0.71073	0.71073	0.71073
color and habit	red-green, blocks	orange, plates	red, blocks	red, blocks	brown, blocks
T (K)	293(2)	120(2)	293(2)	150(2)	150(2)
reflns collected	5891	14673	32947	10057	25504
reflns/restraint/params	3922/0/283	3177/0/244	12990/0/874	3906/0/310	7173/0/526
D_{calcd} (Mg m^{-3})	1.508	1.692	1.440	1.617	1.479
μ (mm^{-1})	0.827	1.030	0.769	0.742	0.537
GOF on F^2	1.094	0.927	1.054	1.043	0.930
final R indices $I > 2\sigma(I)$[a]	R1 = 0.0387	R1 = 0.0260	R1 = 0.0563	R1 = 0.0200	R1 = 0.0278
	wR2 = 0.0994	wR2 = 0.0510	wR2 = 0.1684	wR2 = 0.0489	wR2 = 0.0591
R indices(all data)[a]	R1 = 0.0424	R1 = 0.0466	R1 = 0.0758	R1 = 0.0241	R1 = 0.0449
	wR2 = 0.1030	wR2 = 0.0541	wR2 = 0.1840	wR2 = 0.0497	wR2 = 0.0621

[a] $R_1 = \sum||F_o| - |F_c||/\sum|F_o|$; $R_2 = \{\sum[w(F_o^2 - F_c^2)^2]/\sum[wF_o^4]\}^{1/2}$.

Table 2. Important Geometrical Parameters of Complexes **1**−**3**, **9**, and **11**

	1	**2**	**3**	**9**	**11**
Ru−N1	2.077(3)	2.081(2)	2.075(4)	2.0788(15)	2.0783(17)
Ru−N2	2.075(3)	2.081(2)	2.070(4)	2.0766(16)	2.0797(19)
Ru1−C_{av}(arene)	2.194	2.179	2.196	2.203	2.246(2)
Ru1−Cl1/N3/P1	2.4226(8)	2.4194(8)	2.3982(15)	2.1185(17)	2.0797(19)
N1−O1			1.179(10)	1.234(3)	1.227(3)
N1−O2			1.220(10)	1.216(2)	1.226(3)
C=N	1.142(5)	1.130(4)			
N2−Ru1−N1	84.86(12)	86.79(9)	85.70(17)	86.45(6)	86.85(7)
N2−Ru1−Cl1/N3/P1	87.83(9)	84.68(7)	85.91(13)	85.07(7)	88.04(5)
N1−Ru1−Cl1/N3/P1	86.72(9)	83.87(7)	87.14(13)	86.63(6)	86.62(5)
C13−N3−O2/O1	175.8(4)		117.0(8)	118.99(19)	118.1(2)
O1−N1−O2			123.2(8)	123.13(18)	124.0(2)
C13/19−C14/20−N3	175.8(4)	174.4(5)			
N2−Ru1−N1−C6/C4	23.3(3)	−9.6(2)	13.4(4)	−13.28(17)	−14.11(18)
N1−Ru1−N2−C4/C6	−27.6(3)	7.4(2)	−15.0(5)	10.55(17)	16.93(19)
C4/C6−C5−C10−C11(phenyl)	113.3(4)	91.0(4)	70.3(7)	91.5(2)	67.6(3)
C14−C13−N3/N6−O1/O2(NO2)			−5.5(14)	1.5(3)	14.7(3)
C15−C13−C14−N3 (C=N)	174.62	158.01			

corresponding to $\nu(N_3)$ and ν(SCN). It suggested linkage of N_3^- and SCN^- to the metal center which has further been established by structural studies. Analogous trends have been observed in the IR spectra of **9** and **10**. The complexes containing PPh_3, $AsPh_3$, dppm, and 4,4′-bipyridine (**8**, **11**, **12**, **13** and **14**) in its IR spectra also exhibited characteristic bands associated with the respective ligands and counter-anion $SO_3CF_3^-$.

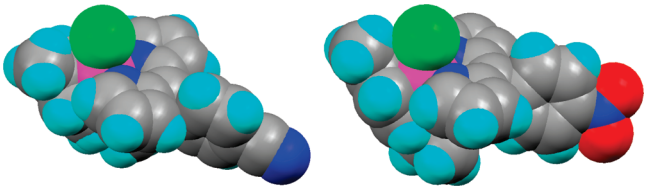

Figure 1. Space-filling representations of [(η^6-$C_{10}H_{14}$)RuCl(ndpm)] **3** (left) and [(η^6-$C_{10}H_{14}$)RuCl(cydpm)] **1** (right).

Crystallographic Studies on Derivatives of the Arene Ruthenium Dipyrrinato Complexes. Molecular structures of the complexes **9** and **11** have been determined crystallographically. Details about data collection, refinement, and structure solution are summarized in Table 1, and selected geometrical parameters are recorded in Table 2. ORTEP views at 30% thermal ellipsoid probability are depicted in Figure 2. The asymmetric unit of **9** contains one ruthenium bonded to nitrogen atoms of the dipyrrin, nitrogen from azide and *p*-cymene ring in η^6-manner resulting in *piano stool* geometry about the metal center. The Ru(1)−N(1) and Ru(1)−N(2) (dipyrrin) distances are 2.0788(15) and 2.0766(16) Å, respectively, which vary by 0.006 Å from the precursor complex **3**. The Ru(1)−N(3) distance (azide) is 2.118 Å, and is comparable to the Ru−N distances reported in the literature.[15a,15f] The average Ru−C(arene) distance is 2.203 Å, which is slightly longer (0.007 Å) compared to that in the precursor complex **3**.

Scheme 2. Synthesis of Mono-/Bi-Nuclear Complexes (i) NaN_3/Acetone, (ii) NH_4SCN/Acetone, (iii) $AgSO_3CF_3/PPh_3$/Acetone, (iv) $AgSO_3CF_3$/L-L/Acetone, and (v) NaN_3/Acetone

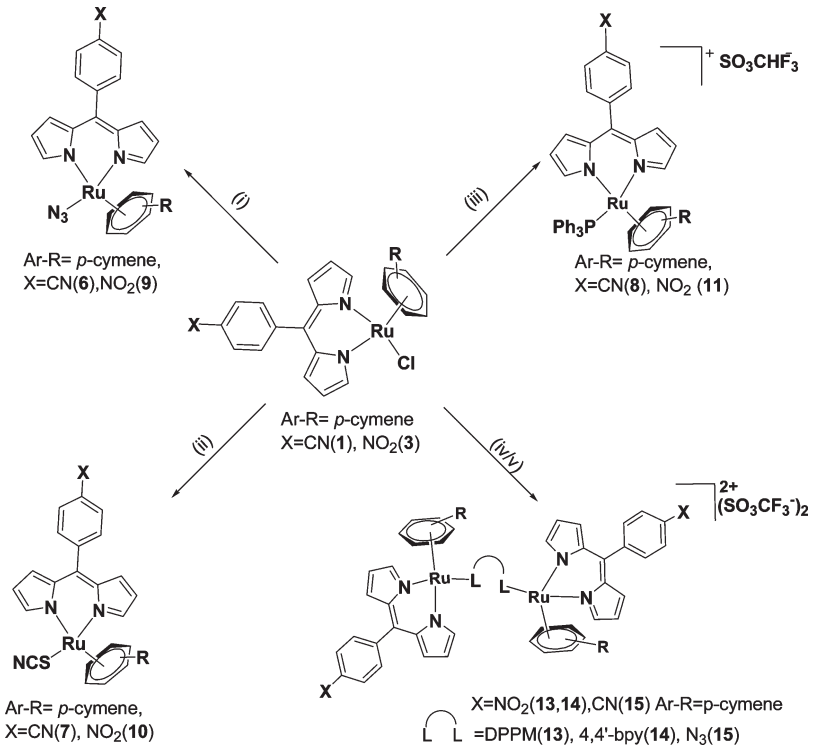

Lengthening of this distance may result from replacement of Cl^- by the bulkier N_3^- group. The separation between ruthenium to the centroid of the *p*-cymene ring is 1.684 Å and is comparable to that in the precursor complex **3** (1.678 Å). The N−Ru−N angle is 86.45(6)° which is slightly larger than in the complex **3** (85.70(17)° and smaller than that in most of the other dipyrrin complexes based on 3d metals.[6,28] The phenyl ring is perpendicular to the methene plane with a dihedral angle of 91.5(2)°.

In complex **11** the metal center ruthenium is bonded with the dipyrrin nitrogen N(1) and N(2), P(1) from PPh_3 and *p*-cymene ring in η^6-manner. Considering the *p*-cymene ring as a single coordination site, the overall geometry about the ruthenium center might be described as *piano-stool* geometry. The *p*-cymene ring in this complex is almost planar, and ruthenium is displaced from the centroid of the *p*-cymene ring by 1.749 Å. It is longer than that in the precursor complex **3** (1.678 Å). The angle N(1)−Ru(1)−N(2) is 86.85°, which is almost the same [86.45(6)°] as that in complex **9** (Table 2). However, the Ru−N bond distances in **11** (2.077−2.079 Å) are comparable to those in the complexes **3** and **9**. Substitution of the Cl^- by bulky ligands PPh_3 (**9**) and N_3^- (**11**) leads to lengthening of the Ru-*p*-cymene separations [Ru−C(average), Ru-centroid; 2.203, 1.684 (**9**) and 2.246, 1.749 Å (**11**)] in comparison to that in the precursor complex **3** (2.196, 1.678 Å). Like other complexes, pyrrole rings within the dipyrrin moiety are not coplanar, rather the mean planes of the two rings intersect at an angle of 21.25(27)° in complex **11**. The C−H···N, C−H···O interactions [Supporting Information, Table S1] in **9** and **11** lead to various structural motifs shown in the Supporting Information, Figures S13,15−16.

(28) Heinze, K.; Reinhart, A. *Inorg. Chem.* **2006**, *45*, 2695–2703.

NMR Spectral Studies. ^{1}H NMR spectral data of the complexes are summarized in the Experimental Section. To facilitate assignments ^{1}H−^{1}H COSY experiments were performed, and the resulting spectra for **1** and **3** are depicted in the Supporting Information, Figures S14−17. The electron withdrawing or donating nature of the phenyl substituents exhibited a pronounced effect on the position of the resonances corresponding to various protons of the coordinated dipyrrins. The α-pyrrolic protons of the dipyrrins in the complexes exhibited significant deshielding (~δ 8.03 ppm) as compared to that in the respective dipyrrins, while β-protons appeared as doublets of doublets in the complexes having electron withdrawing substituents (−CN, $-NO_2$) and as two well resolved doublets (see in Supporting Information, Figure S18) in the complexes containing the electron releasing group $-OCH_2Ph$. Comparative results demonstrate that, although β-protons are magnetically different, resonances associated with them appear as doublets of doublets on the NMR time scale. The combined effect of the coordination of pyrrolic nitrogen to ruthenium and the nature of the *meso*-substituent (electron withdrawing or releasing) of dipyrrins determines the position of doublets corresponding to β-protons. Further, space filling models of **1** and **3** show that steric interaction between α-pyrrolic protons and η^6-aromatic ring current and the additional electron withdrawing effect imposed by ruthenium on adjacent nitrogen leads to greater deshielding of α- relative to β-protons.[10c] For example in the ^{1}H NMR spectrum of **1**, signals associated with the cydpm protons resonated at δ 6.45 (d, 2H, J = 4.8 Hz, β-H py), 6.49 (d, 2H, J = 4.8 Hz, β-H py), 7.50 (d, 2H, J = 6.6 Hz, phenyl), 7.71 (d, 2H, J = 8.1 Hz, phenyl), 8.03 (s, 2H, α-H py) ppm. An analogous pattern of the resonances have been observed in the spectrum of **2**. The resonances associated with *meso*-substituted phenyl protons of the

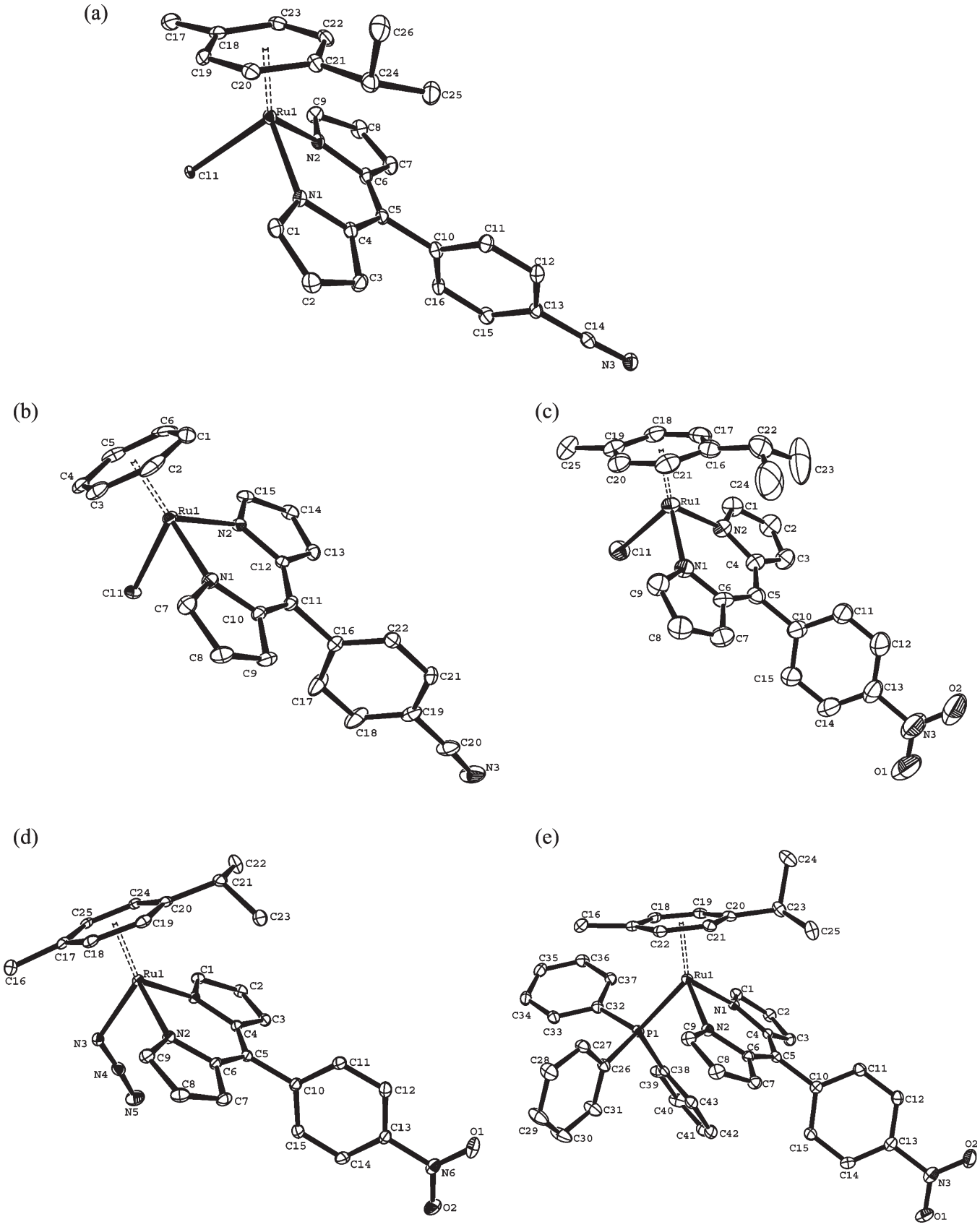

Figure 2. ORTEP diagrams of **1**(a), **2**(b), **3**(c), **9**(d), and **11**(e) at 30% thermal ellipsoid probability (H-atoms omitted for clarity).

dipyrrin (ndpm) in **3** and **4** were relatively deshielded. It may be attributed to the strong electron withdrawing nature of the nitro group. The $^{1}H-^{1}H$ COSY experiments showed that two types of phenyl protons are interacting with each other. Protons associated with dipyrrin (bdpm) in **5** were displayed in the range δ 5.12−7.99 ppm. Further, protons

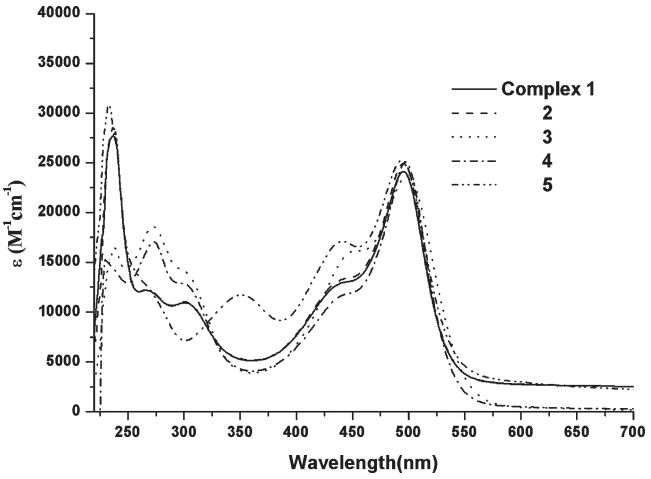

Figure 3. Electronic spectra of **1**−**5** in dichloromethane.

associated with the coordinated *p*-cymene (**1**, **3**, **5**) and benzene (**2**, **4**) resonated at δ 1.10 (d, 6H, $CH(CH_3)_2$, J = 6.9 Hz), 2.24 (s, 3H, $C-CH_3$), 2.40 (m, 1H, $CH(CH_3)_2$), 5.30 (dd, 4H, C_6H_4), and 5.68 (s, 6H, C_6H_6) ppm, respectively.[16] Signals associated with the arene protons exhibited an insignificant shift in these complexes. Substitution of the Cl^- by various ligands from precursor complexes **1** and **3** causes splitting and deshielding of the various signals associated with dipyrrin and arene protons. It may be attributed to the change in electron density on the metal center because of the linkage of the displacing ligands.

Electronic Spectroscopy. UV−vis spectra of the complexes were recorded in dichloromethane, and the resulting data is summarized in the Experimental Section. The electronic spectra of **1**−**5** (Figure 3) exhibited moderately intense bands at ∼ 400−500, 301, 267, and 237 nm. Highly conjugated dipyrrin complexes usually display intense bands in the range of 400−500 nm corresponding to dipyrrin-based $S_0 \rightarrow S_1$ ($\pi \rightarrow \pi^*$) transitions[6e,9c,10c] along with metal-dipyrrin charge transfer transitions in the visible region.[10c,21,29] High energy transitions have been tentatively assigned to intraligand transitions associated with the dipyrrins.[6e,8a,19c,21,23] In complex **5**, bands at 350 nm exhibited a red shift in comparison to the complexes **1**−**4** (∼305 nm). This shift may be attributed to the presence of the benzyloxy chromophore. It was further observed that substitution of the Cl^- in complexes **1** and **3** by neutral or anionic ligands (PPh_3, N_3^-, SCN^-) resulted in a small blue shift in the position of the absorption bands. The electronic spectra of the binuclear complexes did not show any appreciable shift in the position of the lowest energy transition bands.

Emission Spectroscopy. Emission experiments on the complexes were carried out in DCM with 1.0 mM solutions at RT Upon excitation at their respective lowest energy bands these complexes did not exhibit any emission (detection limit = 0.1%). Most of the complexes containing dpm reported in the literature exhibit strong fluorescence.[6a] Quenching of the fluorescence in the complexes under study is a matter of discussion. The absence of the fluorescence may be attributed to non-rigidity of the *meso*-phenyl rings of dipyrrins, which may lead to deactivation of the excited state.[9b] We do not have any strong evidence to suppot the observation at this stage. The possibility for deactivation of the excited state via some other non-radiative energy transfer pathway can not be ruled out. However, these results are consistent with the observations made by Lindsey and coworkers on some other systems.[30,31]

Mass Spectrometry. The FAB-Mass spectra of the complexes **4**, **5**, **8**, **12**, **13**, and **15** provided valuable information about relative stability of various moieties and supported formation of the respective complexes. The FAB-Mass spectrum of **4** displayed peaks at m/z 478(478.9), 443(443.4), 365(365.3), and 265(264.2) assignable to $[M^+]$, $[M^+ - Cl]$, $[M^+ - (Cl + benzene)]$, and $[L^+]$, respectively, while, that of **5** exhibited peaks at m/z 595(596.1), 560(560.7), 426(426.5), and 468(469.5) assignable to $[M^+]$, $[M^+ - Cl]$, $[M^+ - (Cl + p\text{-cymene})]$, $[M^+ - (Cl + CH_2{-}Ph)]$, respectively. The overall fragmentation pattern and relative abundance of the various peaks in the FAB-MS spectra of **4** and **5** indicated that the arene ligand is loosely bonded to the ruthenium center in comparison to the dpm ligands. Ionic complexes **8** and **12** in their FAB-mass spectra displayed molecular ion peaks (resulting from loss of the counterion $SO_3CF_3^-$) at m/z 741(741.8) and 805 (805.8), respectively. The loss of the coordinated PPh_3 or $AsPh_3$ in the next step is supported by the presence of the peaks at m/z 479(479.6) and 499(499.5), respectively. This step is followed by loss of the arene ligand *p*-cymene, which is further supported by the presence of the peaks at m/z 345(345.4) and 365(365.3). Formations of the binuclear complexes were also strongly supported by the FAB-MS spectral studies. Peaks observed at 1532(1532.5), 1113(1115.1), 883(883.9), 749(749.7), and 499(499.5) in the spectrum of **13** conformed well to its dinuclear formulation. The fragmentation pattern of **15** (Figure 4), which displayed peaks at m/z 999(999.1), 479(479.6), 345(345.4), 244(244.2) also, corresponded well to its dinuclear formulation.

Electrochemical Studies. Redox properties of the complexes **1**, **3**, **5**, **9**, **11**, and **14** have been followed by cyclic voltammetry. The resulting data is summarized in Table 3, and a representative voltammogram for **1** is depicted in Figure 5. The potential of the Fc/Fc^+ couple under the experimental conditions was 0.10 V (80 mv) vs Ag/Ag^+. Neutral and cationic species exhibited one electron oxidation corresponding to the Ru(II)/Ru(III) redox couple (Table 2) in the potential range of 0.80−0.98 and 0.96−1.26 V vs Ag/Ag^+.[16a,32] Data on the complexes **1**, **3**, and **5** suggested that the oxidation potentials are affected by the electron withdrawing/donating ability of *meso*-substituents of the dipyrrin ligands. Electron-donating groups (benzyloxy, **5**) increases electron density on the ligand and also the ruthenium center, which in turn leads the redox

(29) Halper, S. R.; Stork, J. R.; Cohen, S. M. *Dalton Trans.* **2007**, 1067–1074.

(30) Sazanovich, I. V.; Kirmaier, C.; Hindin, E.; Yu, L.; Bocian, D. F.; Lindsey, J. S.; Holten, D. *J. Am. Chem. Soc.* **2004**, *126*, 2664–2665.

(31) Sutton, J. M.; Rogerson, E.; Wilson, C. J.; Sparke, A. E.; Archibald, S. J.; Boyle, R. W. *Chem. Commun.* **2004**, 1328–1329.

(32) (a) Lever, A. B. P. *Inorg. Chem.* **1990**, *29*, 1271–1285. (b) Lever, A. B. P. In *Comprehensive Coordination Chemistry II*, Lever, A. B. P., Ed.; Elsevier Science: Oxford, U.K., 2004; Vol. *2*, Chapter 2.19, pp 251−268 and references therein. (c) Pombeiro, A. J. L. In *Encyclopedia of Electrochemistry*; Scholz, F., Pickett, C. J., Eds.; Wiley-VCH: New York, 2006; Vol. *7A*, Chapter 6, pp 77−108 and references therein. (d) Reisner, E.; Arion, V. B.; Eichinger, A.; Kandler, N.; Geister, G.; Pombeiro, A. J. L.; Keppler, B. K. *Inorg. Chem.* **2005**, *44*, 6704–6716.

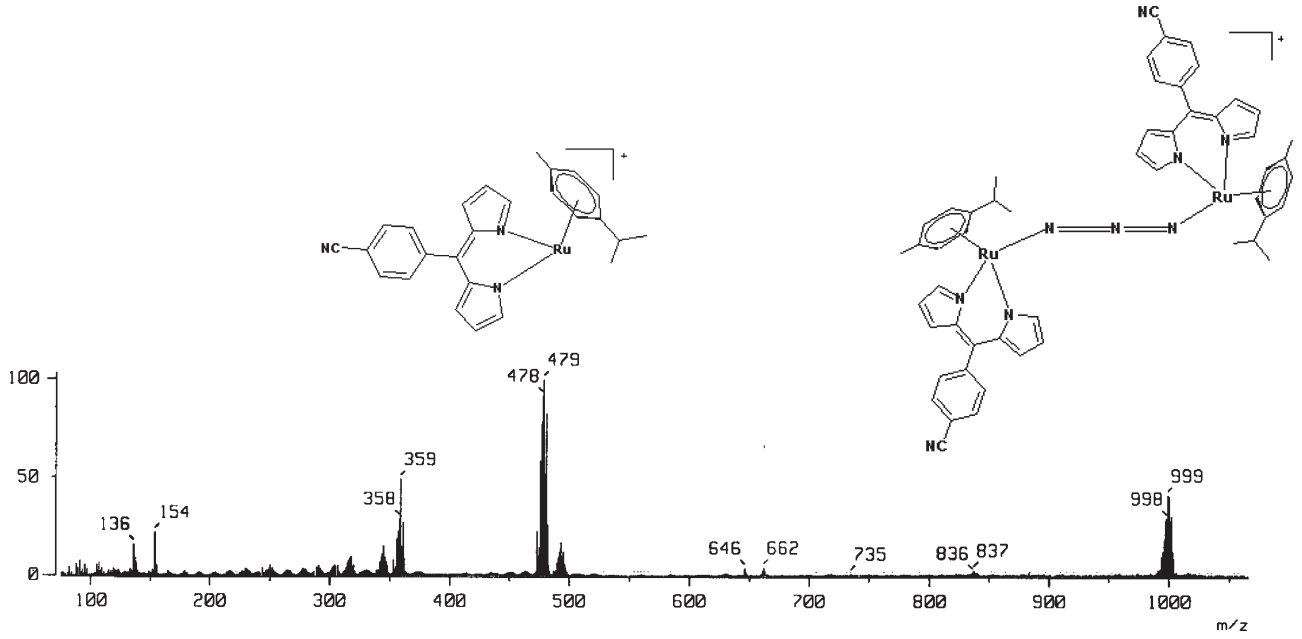

Figure 4. FAB mass spectra of **15**.

Table 3. Cyclic Voltammetric Data for Arene Ruthenium(II)-dpm Complexes

complexes	$E°_{ox}$, V (ΔE, mV)	$E°_{ox}$, V (ΔE, mV)
Fc	0.10(80)	
1	0.82(89), 0.71	−0.25, −1.44, −1.52(73)
3	0.98(110), 0.83	−0.18, −0.99, 1.11[b], −1.26[b]
5	0.80(94), 0.67	−0.09, −0.27, −1.10, −1.23(62), −1.55, −1.61(68)
9	0.88(78), 0.65	−0.36[a], −1.17, −1.38(26)
11	0.96(115), 0.75, 0.54	−0.26, −1.28[b]
14	1.26[a], 0.85, 0.27[a]	−0.42, −1.16(94), −1.25[b]

[a] = peak potentials, $E_{p,a}$ for irreversible processes. [b] = quasi-reversible processes.

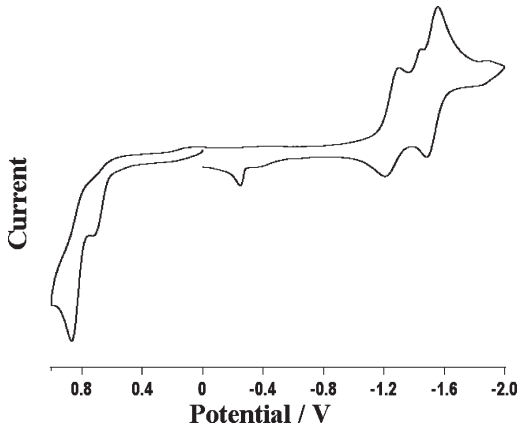

Figure 5. Cyclic voltammogram of **1**.

process to occur at more negative potentials, while the opposite effect occurs when electron withdrawing groups are employed. The value of the Ru(II)/Ru(III) oxidation potential in the complexes under study reflects the electron-donor behavior of the ligands as follows: Replacement of chloride in complex **3** by azide to form **9** results in a measurable shift (although rather small) in the cathodic potential (from + 0.98 to + 0.88 V), which is in keeping with slightly better electron donor properties of the latter.[32a] In contrast, substitution of Cl^- by PPh_3 to form **11** is expected to result in a measurable anodic shift in the oxidation potential, but a measurable shift was not observed. However, replacement of Cl^- by 4,4′-bpy to form **14** (from + 0.98 to +1.26 V).[33] leads to an appreciable potential shift. The presence of a single oxidation wave (at $E_{p,a}$ 1.26 V) corresponding to Ru(II)/Ru(III) in the binuclear complex **14** suggested lack of electronic communication between the two ruthenium centers through the bridging ligand.[32,34] All the complexes exhibited an additional oxidation wave with lower current intensity at a potential of about 0.65−0.85 V. This may be attributed to the oxidation of dipyrrin which falls within the range for the dipyrrin complexes.[6a,22,35,36] Reduction of the complexes shows two well resolved quasi-reversible peaks (some complexes shows reversible peaks) in the potential range 0.00 to −2.00 V; this is expected because of the reduction of dipyrrins.[6a,22,35,37]

Spectroelectrochemistry. The UV/vis spectra and redox potentials of **1**, **3**, and **5** do not differ much; therefore, complex **3** and its derivative **11** along with one of the binuclear complexes **14** were chosen for spectroelectrochemical studies. The studies were performed in acetonitrile solution

(33) (a) Sullivan, B. P.; Salmon, D. J.; Meyer, T. J. *Inorg. Chem.* **1978**, *17*, 5239. (b) Kaim, W.; Reinhardt, R.; Sieger, M. *Inorg. Chem.* **1994**, *33*, 4453–4459.

(34) Bröring, M.; Brandt, C. D.; Bley-Escrich, J.; Gisselbrecht, J. P. *Eur. J. Inorg. Chem.* **2002**, 910–917.

(35) (a) Gill, H. S.; Finger, I.; Bozidarevic, I.; Szydlo, F.; Scott, M. J. *New J. Chem.* **2005**, *29*, 68–71. (b) Cui, A.; Peng, X.; Fan, J.; Chen, X.; Wu, Y.; Guo, B. *J. Photochem. Photobiol. A: Chem.* **2007**, *186*, 85–92. (c) Goze, C.; Ulrich, G.; Ziessel, R. *J. Org. Chem.* **2007**, *72*, 313–322.

(36) (a) Bröring, M.; Brandt, C. D.; Lex, J.; Humpf, H. U.; Bley-Escrich, J.; Gisselbrecht, J. P. *Eur. J. Inorg. Chem.* **2001**, 2549–2556. (b) Rawling, T.; Xiao, H.; Lee, S. T.; Colbran, S. B.; McDonagh, A. M. *Inorg. Chem.* **2007**, *46*, 2805–2813. (c) Kadish, K. M.; Shao, J.; Ou, Z.; Frèmond, L.; Zhan, R.; Burdet, F.; Barbe, J.-M; Gros, C. P.; Guilard, R. *Inorg. Chem.* **2005**, *44*, 6744–6754.

(37) (a) Tabba, H. D.; Cavaleiro, J. A. S.; Jeyakumar, D.; Graca, M.; Neves, P. M. S.; Smith, K. M. *J. Org. Chem.* **1989**, *54*, 1943–1948. (b) Bröring, M.; Brandt, C. D.; Bley-Escrich, J.; Gisselbrecht, J. P. *Eur. J. Inorg. Chem.* **2002**, 910–917. (c) Falk, H.; Leodolter, A.; Schade, G. *Monatsh. Chem.* **1978**, *109*, 183–192.

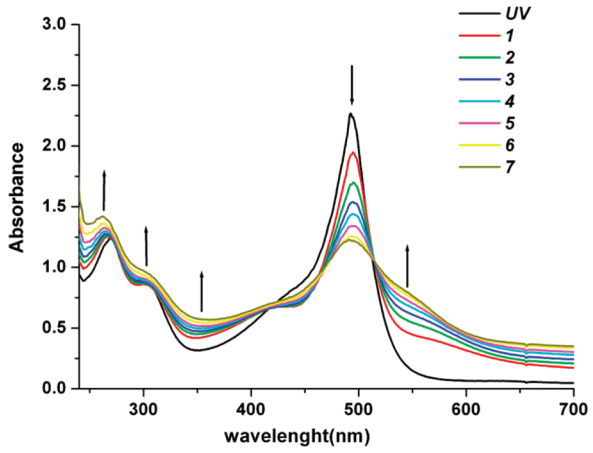

Figure 6. Electronic spectra of **3** in acetonitrile upon applying oxidizing potential.

Table 4. Electronic Transition Data on Applying Potential

complexes	peak positions (oxidized species)
3	240, 263, 301, 423, 493, 542(sh)
11	253, 310, 444, 496−486
14	263, 294, 424−416, 496−487, 537(sh)

at RT. A representative spectrum for **3** is depicted in Figure 6, while those of **11** and **14** are shown in the Supporting Information, Figures S8−9, and the resulting data are summarized in Table 4. Oxidative spectroelectrochemistry was performed with an applied potential of 1.20 V for (**3**, **11**) and 1.40 V for **14**. After oxidation, regenerated radical cations of the respective complexes were followed by a shift in the position of bands and the appearance of a shoulder in the optical spectra. Electrogenerated species exhibited broad absorption bands with low absorbance. The UV/vis spectra of complexes **11** and **14** also, displayed changes upon oxidation, and electrogenerated species displayed analogous trends within the series (Supporting Information, Figures S8−9). Broadening of the absorption bands were observed during oxidation. Further, the lowest energy band weakened significantly and a shoulder appeared in the lower energy region. This behavior may be attributed to the metal-dipyrrin centered redox reactions. The peaks below 301 nm exhibiting only a slight increase in the intensity of transition bands have been assigned to the dpm based transitions. Appearance of a shoulder at 542 (**3**) and 537 nm (**14**) upon oxidation was slightly blue-shifted and attains some intensity upon generation of the Ru(III) species.

Conclusions

In summary, in this work we have reported syntheses and characterizations of a series of heteroleptic ruthenium complexes containing both the dipyrrin and the arene ligands. New series of *piano-stool* complexes with the general formulations [(η^6-arene)RuCl(dpm)] (η^6-arene = C_6H_6, $C_{10}H_{14}$) represent first examples of complexes imparting both the dipyrrin and the arene ligands. The reactivity of the resulting complexes have been examined with various bases to afford substitution products [(η^6-arene)Ru(dpm)X] (X = N_3^-, SCN^-) and [(η^6-arene)Ru(dpm)(EPh_3)]$^+$ (E = P, As). Chelation of the dipyrrin ligands through pyrrolic nitrogen have been authenticated crystallographically. In addition, some bimetallic complexes have also been synthesized and characterized by analytical and spectral studies.

Acknowledgment. Thanks are due to the Council of Scientific and Industrial Research, New Delhi, India for providing financial assistance through the schemes [HRDG 01(2074)/06/EMR-II] and [HRDG 01(2097)/07/EMR-II] (partial assistance). We also thank the Head, SAIF, Central Drug Research Institute, Lucknow for extending FAB mass spectral data and Prof. P. Mathur, In−charge, National Single Crystal X-ray Diffraction Laboratory, Indian Institute of Technology, Powai, Mumbai, for X-ray facilities.

Supporting Information Available: Figures S1−S21, full crystallographic data in CIF format for the structure determinations of **1**, **2**, **3**, **9**, and **11** and Table S1. This material is available free of charge via the Internet at http://pubs.acs.org.